doi:10.1016/j.jmb.2008.01.060 J. Mol. Biol. (2008) 377, 1002–1014

JMB

Available online at www.sciencedirect.com

ScienceDirect

ELSEVIER

# Accurate Genetic Switch in *Escherichia coli*: Novel Mechanism of Regulation by Co-repressor

**Marcin Tabaka[1], Olgierd Cybulski[1] and Robert Hołyst[1,2]***

[1]*Institute of Physical Chemistry, Polish Academy of Sciences, Kasprzaka 44/52, 01-224 Warsaw, Poland*

[2]*Department of Mathematics and Natural Science, College of Sciences, Cardinal Stefan Wyszynski University, 01-815 Warsaw, Poland*

*Received 22 September 2007; received in revised form 27 December 2007; accepted 15 January 2008*
Available online 31 January 2008

***Edited by J. Karn***

Understanding a biological module involves recognition of its structure and the dynamics of its principal components. In this report we present an analysis of the dynamics of the repression module within the regulation of the *trp* operon in *Escherichia coli*. We combine biochemical data for reaction rate constants for the *trp* repressor binding to *trp* operator and *in vivo* data of a number of tryptophan repressors (TrpRs) that bind to the operator. The model of repression presented in this report greatly differs from previous mathematical models. One, two or three TrpRs can bind to the operator and repress the transcription. Moreover, reaction rates for detachment of TrpRs from the operator strongly depend on tryptophan (Trp) concentration, since Trp can also bind to the repressor–operator complex and stabilize it. From the mathematical modeling and analysis of reaction rates and equilibrium constants emerges a high-quality, accurate and effective module of *trp* repression. This genetic switch responds accurately to fast consumption of Trp from the interior of a cell. It switches with minimal dispersion when the concentration of Trp drops below a thousand molecules per cell.



*Keywords:* *trp* operon; genetic switch; transcriptional regulation; repressor control

## Introduction

Regulation of the tryptophan (Trp) operon in *Escherichia coli* is one of the most exhaustively studied gene control systems both experimentally[1–4] and theoretically.[5–14] The regulation is achieved by means of two mechanisms controlling successive stages of expression: repression[15,16] and attenuation.[17,18] These mechanisms allow the bacterium to monitor the intracellular concentration of Trp and respond efficiently to nutritional changes in environment. Repression regulates initiation of transcription by blocking attachment of RNA polymerase (RNAP), while attenuation is responsible for premature termination of transcription due to conformational changes in mRNA.

The repression is achieved by attachment of an active tryptophan repressor (TrpR) to the operator and masking RNAP recognition sequence.[19] The TrpR is a small (25 kDa) protein consisting of two 107-amino-acid chains.[20–22] The repressor is activated by non-cooperative binding of two Trp molecules.[23–26] The active repressor is called holorepressor. Both X-ray[27–29] and NMR[30–32] studies of non-active and active repressors have revealed that this protein belongs to the helix–turn–helix (HTH) family. The binding of Trp causes allosteric transitions that stabilize the HTH reading heads and change the distance between them. These heads of holorepressors make contact with two successive major grooves of DNA at the operator.

Structural[33–35] and DNA footprinting analyses[36–38] of the operator–repressor complexes pointed to the sequence 5′GNACT′3′ as being crucial for specific binding. This half-site and its reflection with a spacer of eight base pairs creates a complete motif for HTH recognition. Interestingly, there is only one direct hydrogen bond between the repressor and a guanine base of DNA at half-site. The contact between protein and DNA is mediated mainly through water molecules[39,40] and phosphate interactions. Moreover, DNA is bent in each half-site,[41,42] and

**Corresponding author.* Institute of Physical Chemistry, Polish Academy of Sciences, Kasprzaka 44/52, 01-224 Warsaw, Poland. E-mail address: holyst@ptys.ichf.edu.pl.

Abbreviations used: Trp, tryptophan; TrpR, tryptophan repressor; RNAP, RNA polymerase; HTH, helix–turn–helix.

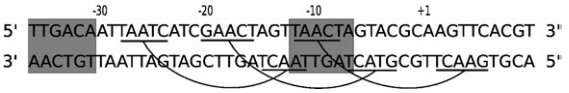


**Fig. 1.** The sequence of the *trp* operator–promoter region. The underlined bases are recognized by repressors. The numbers indicate positions relative to the first transcribed residue (+1). The recognition sequences for RNAP are marked with gray boxes.

this feature is crucial for the ability of the operator to assume a conformation that enables direct hydrogen bonds between protein and phosphate groups. These "non-specific" elements of the operator provide for specific binding of TrpR. Such mode of recognition was termed "indirect readout".[33]

*In vitro* studies demonstrated that the operator may be occupied by three repressor dimers[36–38,43–46] depending on repression conditions. This mode of binding was also confirmed by *in vivo* experiments.[38] A sequence of the operator with marked alignment of *trp* repressors is depicted in Fig. 1. The centered, bound repressor is flanked by two similarly attached repressors without steric hindrance.[35] However, these flanking repressors bind to imperfect half-sites 5′TAACT3′ and 5′TAATC3′ with less affinity than the central one. The first repressor binds to two perfect half-sites (central), while the second one picks out sequences (right) with one mismatched half-site. If the concentration of holorepressors is high, the third dimer binds to two imperfect sites (left).

Due to the indirect recognition and multiple modes of binding, interactions between holorepressors and operator are extremely sensitive to the experimental conditions (length of DNA, buffer compositions, etc.). Therefore, there are many discrepancies in the literature regarding stoichiometry, equilibrium constants and kinetic data for these complexes. For example, equilibrium binding constants for holorepressor/operator differ by 2 orders of magnitude in different experiments.[47,48] Moreover, a common practice among researchers is to use promoters with inappropriate sequences and buffer conditions remote from those encountered in the cytoplasm of *E. coli*.

Trp dissociates rapidly from the repressor–operator complex after its formation.[47,49–51] This process is very fast and leads to destabilization of the complex; however, its stability depends on the concentration of Trp in the medium. Trp can also attach to the complex and thus stabilize it. Therefore, the mean lifetime of the complex depends on the concentration of the co-repressor (Trp). This mechanism allows *E. coli* to respond effectively to a sudden change in the intracellular concentration of Trp, as will be shown here.

Inducible and repressible operons involve a rapid change of expression in response to environmental stimuli. The efficiency of such a switch is determined by its response time to the threshold value of the stimulus. If the stimulus crosses a certain value, gene expression should jump abruptly to maximal level. The efficiency of the *trp* genetic switch is investigated in this report in the framework of the stochastic formulation of chemical kinetics.[52–54] We calculate not only the mean values of system parameters (e.g., on/off switching time of gene expression) but also their distributions. Previous models of regulation of *trp* operon repression[5–14] have not taken into account many repressors binding, the destabilizing effect of co-repressor release and co-repressor rebinding to the repressor–operator complex. We demonstrate here that all these elements of the switch are necessary for accurate response of bacteria to a rapid change of Trp level in a medium. The article is organized as follows: first, we give an outline of our model of the *trp* repression. Next, we study the genetic switch of the *trp* operon subject to Trp changes and discuss the design of the *trp* switch. Finally, we present briefly our methods of computation and present the parameterization of the repression model.

## Model of the *trp* Operon Repression

### Repressor activation

The aporepressor is activated by Trp (co-repressor). This process encompasses binding of two co-repressor molecules to two independent binding sites with identical affinities.[23–26]

$$\mathrm{R} + \mathrm{T} \underset{k_1}{\overset{2k_0}{\rightleftharpoons}} \mathrm{RT} \tag{1}$$

$$\mathrm{RT} + \mathrm{T} \underset{2k_1}{\overset{k_0}{\rightleftharpoons}} \mathrm{RT_2} \tag{2}$$

A list of model variables and symbols is shown in Table 1, while a list of all parameters and their values is presented in the section Methods of Computation. The statistical factor 2 multiplying microscopic reaction rate constants $k_0$, $k_1$ accounts for the fact that there are two identical and independent sites for Trp binding.

Two monomers that form the Trp repressor associate very fast and the repressor dimer is very stable: the half-life of the aporepressor is approximately 50 h.[55] For these reasons we do not take into consideration decay of the dimers and association of the monomers. We assume that the concentration of the dimers is constant and equal to total repressor concentration.

**Table 1.** Nomenclature

| Symbol | Meaning |
|---|---|
| R | Aporepressor |
| T | Tryptophan |
| $RT_2$ | Holorepressor |
| [X] | Concentration of X species |
| $[X_{tot}]$ | Total concentration of X species |
| $O^{(i)}$ | *i*th binding site for the repressor in the operator O |
| P | RNA polymerase |
| $RT_2O^{(i)}$ | Operator occupied at *i*th site by holorepressor |
| PO | Polymerase–promoter complex |
| TC | Transcribing complex |

### Binding of the holorepressors to the operator

The holorepressor binds specifically to the operator site of DNA. Since binding of the holorepressor to non-specific sites are 3 orders of magnitude weaker than the holorepressor binding to the specific site of DNA,[46] we do not consider these processes as being important in promoter blocking. Therefore, the interactions between repressor and operator are described by the equation

$$RT_2 + O^{(1)} \underset{k_3^{(1)}}{\overset{k_2^{(1)}}{\rightleftharpoons}} RT_2O^{(1)} \tag{3}$$

The reaction rate constants $k_2^{(1)}$, $k_3^{(1)}$ (the superscripts differentiate constants for various operator binding sites) and dissociation constant $K_1^{(1)} = k_3^{(1)}/k_2^{(1)}$ strongly depend on experimental conditions. For example, changing the concentration of KCl in a buffer from 0 to 500 mM results in a decrease of $K_1^{(1)}$ by 2 orders of magnitude.[56] There are also discrepancies in $K_1^{(1)}$ determination due to incorrect analysis of data. For example, in many studies a correct sequence of DNA containing three binding sites was used, yet in the determination of $K_1^{(1)}$ it was assumed that only one repressor could bind to the DNA fragment. The length of DNA fragments and mutations in a wild sequence alter bending of the operator and therefore change the affinity and stoichiometry of the repressor–operator interactions. Methods used to measure binding of the repressors to the operator are also of significance. Gel retardation,[37,41,57,58] the method most often used, requires decreasing pH to a non-physiological level, while filter binding assays[47,50,59] cannot distinguish complexes with different stoichiometry. Moreover, all methods in which the concentration of Trp in a buffer changes during experiment give unreliable values of the dissociation constant, because stability of the complexes depends on total Trp concentration (see the next section). A method that does not suffer from the aforementioned disadvantages is fluorescence anisotropy.[46,56] The dissociation constants $K_1^{(1)}$, $K_1^{(2)}$, $K_1^{(3)}$ of the first, second and third holorepressor, respectively, obtained by this method are most reliable and will be used in this work. Equations for binding of the second and third holorepressor are given by:

$$RT_2 + O^{(2)} \underset{k_3^{(2)}}{\overset{k_2^{(2)}}{\rightleftharpoons}} RT_2O^{(2)} \tag{4}$$

$$RT_2 + O^{(3)} \underset{k_3^{(3)}}{\overset{k_2^{(3)}}{\rightleftharpoons}} RT_2O^{(3)} \tag{5}$$

The association of the second repressor is cooperative.[38] One can imagine a situation in which repressors bind first to the second site on the operator. Therefore, it is necessary to take into consideration the constant associated with the cooperativity. Similarly, the third binding site will require another constant. These constants are generally not known. One can overcome these difficulties assuming that repressor binding is sequential. Therefore, the second repressor can bind if and only if the first site has already been occupied. Such approach is justified by the fact that the second binding site is never occupied by the repressor without the repressor at the first binding site.[38] Similarly, the third repressor attaches the operator if the first and second places are bound by repressors. We also assume a sequential unbinding process. This assumption allows one to reduce the number of constants. If the binding site affinities differ significantly and there are strong interactions between proteins on DNA, these assumptions are particularly well justified. The association of the repressor to the third binding site is 2 orders of magnitude weaker than for the first and second binding sites. Therefore, all three operator sites are occupied only at high Trp concentration.

### Tryptophan release

The holorepressor–operator complex quickly releases molecules of Trp,[47,49–51] forming a less stable aporepressor–operator complex. This process was not fully explained and in particular it was not known whether Trp can rebind to the aporepressor–operator complex. There is no doubt that the complex without corepressor is less stable, but, experimentally, the stability of complexes occupied by one or two molecules of Trp has not been differentiated. The experiment performed by Hurlburt and Yanofsky[50] cast light on these problems. These authors measured the dissociation rate of the repressor–operator complex as a function of Trp concentration. They presented their results only graphically without further interpretation. Since the rates are different for various Trp concentrations, we conclude that Trp is able to bind with the repressor–operator complex (if Trp could dissociate only from the repressor–operator complex, these rates should be constant). Therefore, the Trp binding/unbinding process is given by the following equations

$$RT_2O^{(i)} \underset{k_4}{\overset{2k_5}{\rightleftharpoons}} RTO^{(i)} + T \tag{6}$$

$$RTO^{(i)} \underset{2k_4}{\overset{k_5}{\rightleftharpoons}} RO^{(i)} + T \tag{7}$$

The statistical factor has the same meaning as for the repressor activation. We assume that the rate constants $k_4$, $k_5$ are the same for all repressors that are bound with the operator. Since repressor binding is an equilibrium phenomenon, the repressor–operator complexes with one Trp molecule and without any Trps should decay according to the following reaction schemes:

$$RTO^{(i)} \underset{k_6^i}{\overset{k_7^i}{\rightleftharpoons}} RT + O^{(i)} \tag{8}$$

$$RO^{(i)} \underset{k_8^i}{\overset{k_9^i}{\rightleftharpoons}} R + O^{(i)} \tag{9}$$

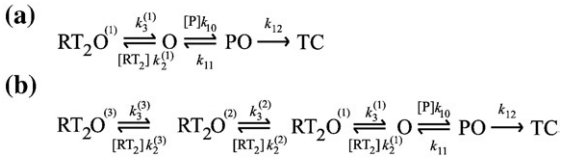


**Fig. 2.** Models of the repression. (a) One binding site for repressor. (b) Three binding sites for repressor.

where superscript $i = 1, 2, 3$ denotes the reaction rate constant for successive repressor–operator complexes. We carefully performed parameterization of the repression model in Methods of Computation.

## Results

In this section we will describe various mechanisms controlling the repression and the process of repressor release from the operator (derepression). First, the regulation is achieved by the change in concentration of holorepressors. Since repressors saturated with Trp can react on the operator with higher affinity, when the concentration of Trp decreases, the pool of available active repressors decreases as well. Two molecules of co-repressor are required for repressor activation, therefore one may expect a sigmoidal type of response to changes in Trp concentration. This mode of regulation is commonly accepted as a main factor of repression. However, since repressors compete with RNAPs for the promoter–operator region, the time that the repressor spends on the promoter should be relatively long in order to efficiently block the transcription initiation. On the other hand, if the Trp concentration decreases below the level required for proper functioning of the bacterium, the response should be instant. This goal is achieved by the second mechanism in which the repressor release from the operator depends on the Trp concentration (the mechanism that was not considered previously in theoretical calculations, yet was observed in experiments[47,49–51]). The third novel mechanism of the repression (many repressors bind to the promoter), not considered previously, accounts for the switch efficiency at high level of Trp concentration. In this case, the gene expression should be completely switched off. In order to accomplish this task, the operator region is blocked by three repressors. We will characterize all mechanisms mentioned above in terms of their efficiency. As a starting point of our calculations, we take a fully repressed state of the repressor–operator complex. The main quantity of interest in calculations is the mean time required for RNAP to bind to the promoter region and start the transcription process. The second quantity of interest, which discerns between a sloppy and accurate genetic switch, is the standard deviation of the binding time. A sloppy switch has a wide time distribution, while an accurate switch has a narrow time distribution of transcription initiation.

### Simplified *trp* switch at constant Trp concentration

Here we present the analysis of the simplified *trp* switch at constant Trp concentration. The simplification relies on neglecting Trp reactions with repressor–operator complex. We also consider only binding of holorepressors to the operator. We calculate mean times required for the RNAP to bind to the promoter and initiate the transcription, assuming that the initial state of the operator is fully repressed, i.e., the operator is bound with the holorepressor(s). Figure 2 depicts models of the repression process. The previous model[5–14] of the process assumes that the repression is gained solely by attachment of the holorepressor to the operator region. In this model (shown in Fig. 2a), the holorepressors bind with the rate constant $[RT_2]\, k_2^{(1)}$, where $[RT_2] = [R_{tot}](1 + k_1 k_0^{-1}[T]^{-1})^{-2}$ is the concentration of holorepressors at a given concentration of Trp. The total concentration of repressors is 120 molecules per cell.[60] The mean time required for transcription initiation $\mu([T])$ (see Methods of Computation and Supplementary Material) as a function of Trp concentration [T] is depicted in Fig. 3 as a continuous line.

Since experiments show that there are three repressor binding sites for *trp* repressor in the *trp* operon, we expect that much longer times are required to free such operator region in comparison to the time needed to free a single binding site in the operator region. The scheme of reactions depicted in Fig. 2b allows one to calculate the time required for RNAP to start transcription. This scheme shows that the repressor–operator complex is stabilized by subsequent binding of the second and third repressors. For such a case, the mean waiting time until the appearance of the reaction PO → TC is shown in Fig. 3 (dashed line).

Three repressors attached to the operator very efficiently block RNAP binding at high Trp concentration. In such a case, there is a 300-fold increase in

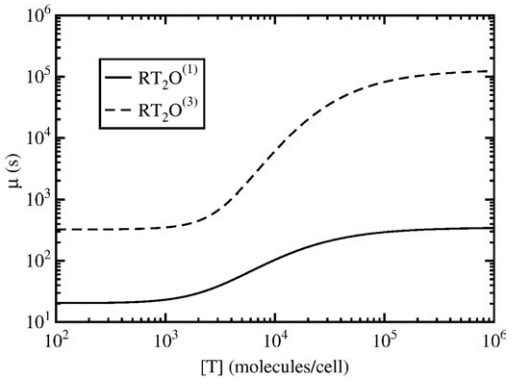


**Fig. 3.** The mean time required for transcription initiation as a function of Trp concentration. The initial state of the operator is completely bound by repressor(s) saturated with two molecules of Trp (as given in the legend). Continuous line, reactions from scheme (a); dashed line, reactions from scheme (b) of Fig. 2.

$\mu([T])$. $RT_2O^{(3)}$, for low Trp concentration, decays quite slowly (about 5 min is needed). This is an effect of the slow dissociation rate for the second repressor. Therefore, one should expect that after rapid Trp uptake, the repressors would still block RNAP binding. That is why destabilization of the repressor–operator complexes is crucial.

### Dynamic response of the *trp* switch to the Trp consumption

Here we present an analysis of the complete *trp* operon repression model presented in this work. The *trp* genetic switch evolved to respond efficiently to changes in the intracellular Trp pool level. Thus, in this section we analyse the response of the switch to changes in the Trp concentration in time. Tryptophan is used in the production of proteins. If a bacterium cannot uptake Trp from the environment, its internal Trp concentration decreases.

We use refined Gillespie algorithm[61] to calculate the mean times required for RNAP to bind to the promoter and initiate the transcription. We also compute the distribution of the transcription initiation times when the concentration of Trp decreases. The simulation steps are as follows: the initial number of free Trp molecules is 50,000 and the concentration of Trp decreases with the rate given by Eq. (21). This decrease is stopped at a certain value of Trp concentration $[T_{fin}]$ (see Fig. 4a). At the beginning of the process the free repressors are fully saturated with Trp and, similarly, operators are fully saturated with repressors. All the reactions discussed in the previous sections are taken into account in the simulations (see also Fig. 7a and b). RNAP binds to the promoter only if all three repressors' binding sites are free. Probability density functions (pdfs) of the transcription initiation times are presented in Fig. 4b for a single repressor binding site within the operator region (as it would be in case of the presence of $O^{(1)}$ only within the operator) and for three binding sites in Fig. 4c. In the case shown in Fig. 4b, repressors cannot efficiently block RNAP binding for high Trp concentrations even for the short time scale considered here. For three repressor binding sites (Fig. 4c), RNAP initiates transcription only when the Trp concentration is very low. In order to characterize the accuracy of the switch that is its response to the various levels of stimulus, one calculates the mean

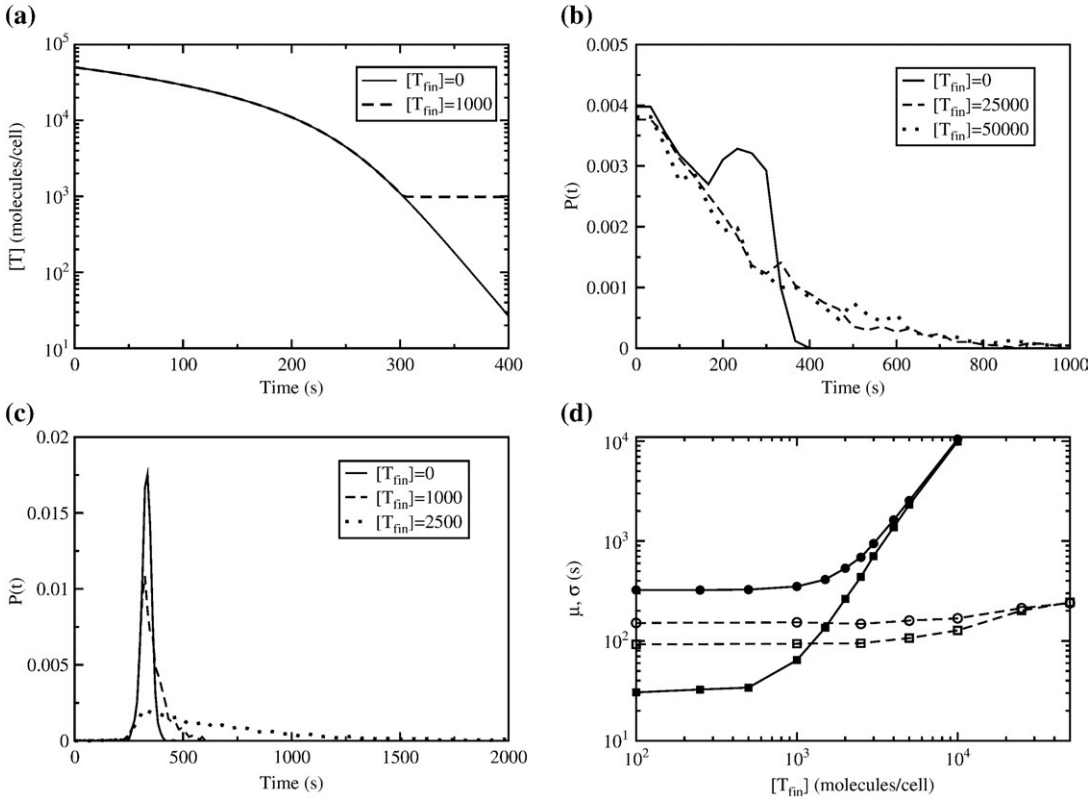


**Fig. 4.** (a) Two examples of Trp concentration changes in time during simulation. In the first case, Trp concentration drops to zero (continuous line) or reaches a small value of 1000 molecules per cell (dashed line). Histograms of RNAP binding times to the promoter for the operator with (b) one binding site and the repressor (c) with three binding sites. During simulations, the Trp concentrations are decreased to the values $[T_{fin}]$ (see insets). The number of independent simulations with the Gillespie algorithm is 2000. (d) Mean times and standard deviations for transcription initiation *versus* concentration of Trp at which its consumption is arrested [see (a). The plot illustrates the accuracy of switching for three repressor binding sites (continuous lines) and for a single repressor (dashed lines). Circles and squares denote mean and standard deviation of the transcription initiation times, respectively.

and the standard deviation for RNAP binding times. The plot of these quantities as a function of Trp concentration at which its consumption is arrested is depicted in Fig. 4d. In the case of the operator with three repressor binding sites, the switch becomes accurate if the Trp concentration decreases below $10^3$ molecules per cell. This is achieved mainly by the process of Trp release from the repressor–operator complexes, because the probability of occurrence of Trp unsaturated complexes increases highly in this range. Above $10^3$ the switch works in a "sloppy" manner. This sloppy mode of action is manifested in a wide time distribution of transcription initiation. Therefore, initiation does not occur with maximum rate if the uptake of Trp is large but does not cross the threshold value. The accurate mode is important for high Trp starvation. In this case, the release of repressor should quickly unblock the operator to initiate polymerase action. These calculations show that the switch dynamically responds to the stimulus, i.e., the accuracy of its reaction depends on the strength of the signal (final Trp concentration). For an operator with only one binding site, the response is actually imperceptible.

In order to investigate the effectiveness of the *trp* switch, we perform also simulations in which the maximum rate of Trp consumption is varied. We use the same initial conditions as described previously. The Trp consumption is continued up to its complete depletion. Figure 5a depicts normalized histograms for transcription initiation times for the case of very slight tryptophan consumption [10 molecules/(cell s)]. The initiation of transcription when only one repressor can block the operator occurs even at high concentration of active repressors. Figure 5a demonstrates that one binding repressor site is not sufficient to compete effectively with RNAPs for the operator–promoter region. We conclude that this mode of regulation is appropriate for genes that maintain approximately constant protein concentration. A good example is *trpR* operon, which contains a single binding site for TrpR within its operator region. Quite a different situation is found when three repressors can bind to the operator, in which RNAP starts to bind significantly only for low Trp level.

The pdfs of transcription initiation times for various values of $V_{\max}$ are depicted in Fig. 5b. We compare the behavior of the *trp* switch for two models of repressor release from the operator. In the first case, the stability of the repressor depends on Trp concentration, and in the second, Trp does not alter decay of the repressor–operator complex. For the latter case and operator with three binding sites, the pdfs are much broader (therefore $\sigma$ is larger) and, generally, RNAPs start binding later [see Fig. 5b, last column, for $V_{\max}=300$ molecules/(cell s)]. Therefore, a simple decay of the repressor–operator complexes would lead to a sloppy response of the *trp* switch to the threshold level of Trp concentration. In such cases, arrest of protein production and slower bacterium division after Trp starvation should be observed. However, these were not

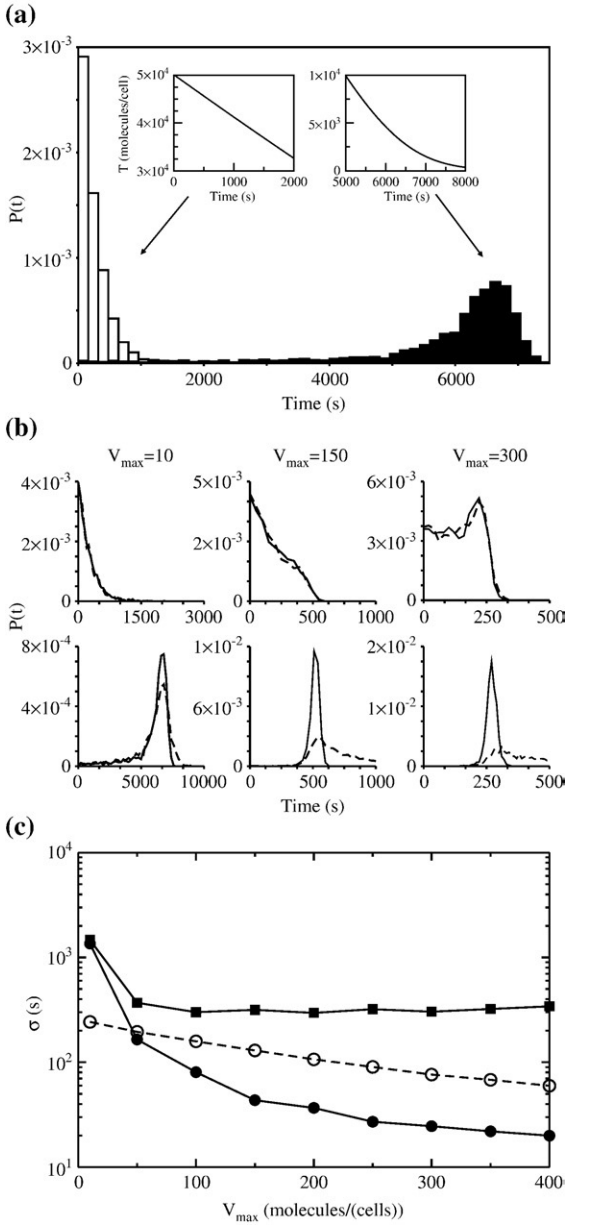


**Fig. 5.** (a) Normalized histograms of transcription initiation times in case of small Trp consumption [10 molecules/(cell s)]. Open bins, repressors can bind only to the operator binding site $O^{(1)}$. Filled bins, repressors can bind to all the operator binding sites $O^{(1),(2),(3)}$. The insets show the Trp concentration at which RNAP binds significantly. (b) Pdfs of the transcription initiation times for various maximum Trp consumptions. The upper graphs are for single binding site within operator region; the lower, for three binding sites. The rates $V_{\max}$ on top are given in molecules/(cell s). Continuous lines represent cases in which Trp can attach to and detach from the repressor–operator complex; dashed lines, Trp cannot bind to/unbind from the complex. (c) Standard deviation for the transcription initiation times as a function of the maximum Trp consumption. Continuous and dashed lines correspond to three and one repressor binding sites, respectively, within the operator. Circles, Trp can attach to/detach from repressor–operator complexes; squares, such a process is absent.

observed in the experiments.[2] Figure 5c sums up all the effects considered here. It presents the standard deviation for transcription initiation times as a function of maximum Trp consumption $V_{max}$ for various models. For an operator with three binding sites, σ decreases because the switch starts responding to a low level of Trp concentration and distributions of times become more accurate. In case of fast Trp uptake, σ is determined mainly by the RNAP reactions (is equal to the mean time required for transcription initiation in case of very low Trp concentration) and is not affected by repressor action, such as is present when stability of the repressor–operator complexes is not regulated by Trp. For one repressor binding case this effect is negligible because the difference in decay rates for $RT_2O^{(1)}$ and $RO^{(1)}$ is too small (therefore, only the case with the regulation of repressor–operator complex stability by Trp is shown in Fig. 5c) Thus, the effectiveness of the switch manifests in the very well defined times for transcription initiation (with very small standard deviation) as the Trp consumption rate grows.

## Summary and Discussion

### Simple explanation of the results

The main result of our study concerns the accurate response of *E. coli* to the change in Trp concentration. When the concentration of Trp reaches $10^3$ molecules per cell, *E. coli* rapidly switches on the *trp* operon. We pointed out that the mechanism responsible for accurate switch is the association–dissociation of co-repressor to the repressor–operator complex. Here we would like to explain this accurate response of *E. coli*. Our reasoning goes as follows: the $RT_2O^{(3)}$ complex, at high Trp concentration and low repressor concentration, decays in 320 s to free the operator. On the other hand, the $RO^{(3)}$ complex decays in 2 s. The dissociation time of the Trp molecule from the RTO complex is 0.3 s. Free holorepressors deactivate about 10-fold faster. Therefore, if the Trp concentration suddenly drops to a very low level, the time for transcription initiation is solely determined by RNAP action. However, for high Trp concentration the binding time for Trp to repressor–operator complex is much faster (for 26,000 molecules per cell it is equal to $5\times10^{-3}$ s) than decay of the repressor–operator complexes. In such a case, binding of Trp stabilizes the whole complex.

This mechanism has another important characteristic. Imagine that the number of free repressors is lower than that used in this work. For example, they are bound to non-specific sites on DNA. If the concentration of Trp is high, all the repressors are saturated with Trp and the $RT_2O^{(2)}$ complex has a large dissociation time. Due to ubiquitous noise, we expect fluctuations of the Trp concentration. Therefore, if the Trp concentration does not drop below $10^3$ molecules per cell, such complex is robust; i.e., it is stable and not affected by spontaneous fluctuations of Trp.

### Biological relevance and predictions of the model

The level of 1000 molecules of Trp per cell is dangerously small for the proper functioning of the bacterium. That is why the accurate response of *E. coli* to the low level of Trp is biologically relevant. This mechanism allows bacteria to synthesize Trp exactly when it is needed. We can make certain predictions at this point concerning cellular population variability. In a population of bacteria that is suddenly brought from Trp-rich medium to Trp-poor medium, we expect bursts of production of proteins that are needed for Trp synthesis. Because the response of *E. coli* is accurate, all bacteria should respond by producing these proteins exactly at the same time (plus or minus a few seconds). In this case, we do not expect large population variability. All bacteria should respond accurately to the stimulus.

Finally, we would like to emphasize that more experiments and theoretical analyses are needed to elucidate the precision and accuracy of the *trp* switch. For example, we could imagine that the relevant switching time is given by the time it takes before newly synthesized protein reaches a certain concentration level. This time would strongly depend on the time it takes to transcribe the operon and translate the mRNA. In order to elucidate this point, full *trp* pathway including attenuation, protein synthesis, their inhibition by Trp, repression of *trpR* operon, degradation of mRNA and Trp proteins, etc. should be included in the model. We plan to do so in the future.

### Detailed balance condition

All the reactions considered here for repressor action are equilibrium reactions, which do not require ATP hydrolysis or other means to overcome the energy barrier. Therefore, for all of them we have to assume the detailed balance condition. This condition is very helpful in the reduction of unknown reaction constants. Not all constants for the *trp* repression have been measured in experiments and some of them had to be either calculated from the detailed balance or assumed. The detailed balance condition also shows the consistency of the reaction scheme and provides verification of experimental results. In Tables 2 and 3, we have explicitly stated which reaction constants have been obtained from the detailed balance condition.

### Further discussion

Our theoretical study based on the Hurlburt–Yanofsky experiment revealed a high-quality, precise and effective module of *trp* repression. We demonstrated that this module responds quickly

**Table 2.** Equilibrium parameters

| | Parameters | | |
|---|---|---|---|
| First repressor | $K_1^{(1)}=0.74$[a] | $K_2^{(1)}=17$[b] | $K_3^{(1)}=380$[b] |
| Second repressor | $K_1^{(2)}=0.64$[a] | $K_2^{(2)}=14$[c] | $K_3^{(2)}=320$[c] |
| Third repressor | $K_1^{(3)}=120$[a] | $K_2^{(3)}=240$[c] | $K_3^{(3)}=2700$[c] |
| Binding of Trp | $K_0=9850$[d] | $K_4=440$[c] | |

[a] Parameters determined by Grillo *et al.*[46]
[b] From Hurlburt and Yanofsky.[50]
[c] Calculated using detailed balance conditions. All dissociation constants are expressed in molecules·per cubic micrometer.
[d] From Schmitt *et al.*[65]

when systematic changes are encountered in the environment and becomes sloppy in the stationary environment, where changes come only from ubiquitous noise. In our article, we demonstrated that the key characteristics of the *trp* repression module is not only the activation and simple binding of TrpR to the operator, but also unbinding of TrpR from the operator. Both processes, binding and unbinding, strongly depend on Trp concentration. Tryptophan release from the repressor–operator complex at low Trp concentration results in a destabilization of the complex. This mechanism allows *E. coli* to respond quickly to the threshold level of Trp concentration. Rebinding of Trp to the complex, at high Trp concentration, allows one to monitor intracellular Trp concentration and stabilize the repressor–operator complex. Finally, we observed that three binding sites for the repressors within the operator are responsible for total blocking of RNAP binding at high Trp concentration.

We do not consider here the role of attenuation—the second mechanism controlling the process of transcription. It was shown that repression is relieved before attenuation.[4] The repression is sensitive to the free Trp pool in the cell, while attenuation is affected by charged $tRNA^{Trp}$ only. The concentration of charged $tRNA^{Trp}$ is adequate to block transcription using attenuation, although there is insufficient amount of Trp molecules in the cell to activate repressors. One should expect that both mechanisms would be responsible for turning on the expression of structural genes when the Trp concentration is very low. It is not surprising that the proteins encoded in the *trp* genes contain few Trp molecules; for example, the anthranilate synthase, the first enzyme produced from structural genes of *trp* operon, contains only two molecules of Trp per 2100 amino acids.

There are many examples showing that operators within the *E. coli* genome consist of many binding sites for repressors. If repression is caused by the steric hindrance of RNAP binding to a promoter, one should expect that the possibility of many repressor binding sites will highly reduce initiation of transcription for sufficient concentration of effectors in the cell. The other mode of repressor action appears when it is bound to an operator. The effector molecules may bind/unbind from the repressor–operator complex and this would induce conformational change of the repressor and alter the stability of the whole complex. As an example, we can give GalR[62] or LacI.[63] Probably this mechanism is common within transcription factors—repressors and activators. The second possible role of the mechanism is protection of the operator from the recurrent rebinding of the same repressor. It was shown[64] that the possibility of the repressor rebinding enhances a noise in the protein production. This is especially important for transcription factors, which bind with operators at a rate close to the diffusion-limited rate. We believe that our accurate description of *trp* repressor module will be helpful in the analysis of other transcription factors in bacteria.

In our article we also described a new method of study of genetic switches. This approach is useful for investigation of response of the switches to constant effector concentration. Such approach allows us to recognize the role and function of individual parts of the switch. Secondly, we changed internal conditions in time to determine the dynamical response of the whole switch. It allows us to understand the functionality of the switch in dynamically changing conditions and its *evolutionary design*.

**Table 3.** Kinetic parameters

| First repressor | Reference | Second repressor | Reference | Third repressor | Reference |
|---|---|---|---|---|---|
| $k_2^{(1)}=0.135$ | $K_1^{(1)}$ | $k_2^{(2)}=5.2\times10^{-3}$ | $K_1^{(2)}$ | $k_2^{(3)}=5.0\times10^{-3}$ | [a] |
| $k_3^{(1)}=0.1$ | Jardetzky and Finucane[66] | $k_3^{(2)}=3.3\times10^{-3}$ | [b] | $k_3^{(3)}=0.6$ | $K_1^{(3)}$ |
| $k_6^{(1)}=0.02$ | $K_2^{(1)}$ | $k_6^{(2)}=7.6\times10^{-3}$ | $K_2^{(2)}$ | $k_6^{(3)}=5.0\times10^{-3}$ | [a] |
| $k_7^{(1)}=0.32$ | [a] | $k_7^{(2)}=0.11$ | [b] | $k_7^{(3)}=1.2$ | $K_2^{(3)}$ |
| $k_8^{(1)}=2.7\times10^{-3}$ | $K_3^{(1)}$ | $k_8^{(2)}=3.4\times10^{-3}$ | $K_3^{(2)}$ | $k_8^{(3)}=5.0\times10^{-3}$ | [a] |
| $k_9^{(1)}=1.0$ | Zhang *et al.*[34] | $k_9^{(2)}=1.1$ | [b] | $k_9^{(3)}=13.5$ | $K_3^{(3)}$ |
| *All repressors* | | | | | |
| $k_0=5.5\times10^{-3}$ | $k_1=54$ | Schmitt *et al.*[65] | | | |
| $k_4=8.1\times10^{-3}$ | $K_4$ | $k_5=3.5$ | Lee *et al.*[51] | | |
| *RNAP binding* | | | | | |
| $k_{10}=6.6\times10^{-2}$ | Sclavi *et al.*[67] | $k_{11}=2.2$ | [b] | $k_{12}=0.12$ | [b] |

First- and second-order rate constants are expressed in units of per second and cubic micrometers per molecule per second, respectively.
[a] Parameters assumed in this work.
[b] Parameters calculated in this work.

## Methods of Computation

### Stochastic treatment of the repression process

The chemical master equation[53] provides a framework for description of chemical reactions. It describes the time evolution of probability that a certain chemical reaction occurs at a given instant of time. As an input, it requires the probability of transition rates, which are normally determined from reaction rates. Although the chemical master equation may be written easily, the analytical or numerical solution exists only for a relatively small number of cases. Therefore, one has to use a numerical description of stochastic chemical kinetics, such as the Gillespie algorithm[52] or its refinements.[61] The algorithm has the following general structure: it attributes to each reaction the probability of occurrence, called propensity function, based on a current state of reagent concentration and the transition rate constants. The propensity function is used to select the occurring reaction and to obtain the time of its occurrence. The time is updated and the procedure is repeated. Advancing this procedure step by step produces a time evolution of chemical reaction systems. It gives the numerical realization of the same stochastic process as described by the chemical master equation. In some simple systems, especially when probability transition rates of reactions do not change in time, the pdf or its moments (mean reaction time, its variance, etc.) can be obtained analytically. Therefore, we present analytical solutions when possible and use modified Gillespie algorithm[61] to obtain numerical solutions in other cases.

For the set of reactions studied here (Fig. 2), we obtain analytical solutions using the following method. Let us assume that the system may leave its initial state, denoted $X_0$, through $N$ channels:

$$X_0 \rightarrow \begin{cases} \xrightarrow{\lambda_1} & X_1, \\ \xrightarrow{\lambda_2} & X_2, \\ \cdots & \\ \xrightarrow{\lambda_N} & X_N \end{cases} \tag{10}$$

with the rate parameters $\lambda_1$ up to $\lambda_N$. The pdf of a waiting time for the transition to occur via any channel is given by

$$P(t) = \lambda \exp(-\lambda t), \quad \lambda = \sum_{i=1}^{N} \lambda_i \tag{11}$$

while a transition via channel $i$ is given by a probability $\lambda_i/\lambda$. The pdf of the transition at time $t+\mathrm{d}t$ through a channel $i$, called *reaction pdf* by Gillespie,[52] is given by:

$$P(t) = \lambda_i \exp(-\lambda t) \tag{12}$$

For $M$ successive reactions:

$$X_0 \xrightarrow{\lambda_1} X_1 \xrightarrow{\lambda_2} \cdots \xrightarrow{\lambda_M} X_M \tag{13}$$

the pdf for occurrence of $M$ reaction at time $t+\mathrm{d}t$ is given by $M$ convolutions of individual pdfs:

$$P(t) = P_1(t)*P_2(t)*\cdots*P_M(t) \tag{14}$$

where

$$P_i(t) = \lambda_i \exp(-\lambda_i t), \qquad \text{for } i = 1,\ldots,M \tag{15}$$

and

$$P_i(t)*P_j(t) = \int_0^t P_i(\tau)P_j(t-\tau)\mathrm{d}\tau \tag{16}$$

After the Laplace transform of Eqs. (11) and (14), the pdfs in the frequency domain take the form

$$f(s) = \sum_{i=1}^{N} \frac{\lambda_i}{s+\lambda} = \frac{\lambda}{s+\lambda}, \qquad \text{for parallel reactions} \tag{17}$$

and

$$f(s) = \prod_{i=1}^{M} \frac{\lambda_i}{(s+\lambda_i)}, \qquad \text{for successive reactions} \tag{18}$$

Such procedure is used for a network of reactions studied in this article (Fig. 2; see Supplementary Material). We write pdf in the frequency domain and obtain the moments, which are the coefficients of pdf Taylor expansion around zero frequency ($s=0$).

### Derivation of model parameters

#### *Equilibrium parameter calculation from detailed balance condition*

All the reactions concerning repressor action considered in this article are equilibrium reactions; that is, they do not require ATP hydrolysis or other means to overcome an energy barrier. The detailed balance imposes constraints on the pathways of dissociation and the values of the dissociation constants. Here, we use detailed balance to calculate dissociation constants that are not determined in experiments. We propose reaction schemes for repressor action as presented in Fig. 6. First we calculate dissociation constants for the reactions of the first repressor. The detailed balance condition for chemical loops states that the overall change of the Gibbs free energy is equal to zero. Therefore, one can write the following equations relating different reaction constants

$$K_0 K_1^{(1)} = K_2^{(1)} K_4 \tag{19}$$

$$K_0 K_2^{(1)} = K_3^{(1)} K_4 \tag{20}$$

Hurlburt and Yanofsky[50] measured the binding of the holorepressor, hemirepressor (one of the monomers has a mutation Gly85-Arg that eliminates Trp

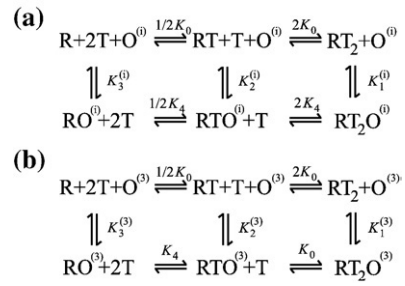


**Fig. 6.** The proposed reaction schemes for repressor action. The scheme for the first and second repressor ($i=1,2$) is presented in (a). (b) The scheme for the third repressor differs from previous schemes in the dissociation constants of Trp and the repressor–operator complex.

binding) and aporepressor. The measured dissociation constants of holo-, hemi- and aporepressors from the operator are at the ratio 1:22.5:500 ($K_1^{(1)}/K_2^{(1)}/K_3^{(1)}$). One can notice that the ratio $K_1^{(1)}/K_2^{(1)}$ is equal to the ratio $K_2^{(1)}/K_3^{(1)}$. It means that we can combine with bottom horizontal reactions the same dissociation constant $K_4$ (the difference is only associated with statistical factors that multiply $K_4$). Therefore, from Eqs. (19) and (20), one can easily obtain $K_4$. All dissociation constants are given in Table 2.

We assume that the scheme of reactions for the second repressor binding with operator $O^{(2)}$ is as for the first repressor. Since only $K_1^{(2)}$ was experimentally determined, we calculated $K_2^{(2)}$, $K_3^{(2)}$ using detailed balance and assume that $K_4$ is the same for both repressors. In the case of the third repressor, $K_1^{(3)}=120$ is much higher than for the first and second repressors and calculation of $K_3^{(3)}$ as previously gives an unrealistic value, which is significantly higher than binding of aporepressor to nonspecific sites on DNA.[46] That is why we assume the scheme of reactions for the third repressor as in Fig. 6b. Here, the repressor that occupies operator $O^{(3)}$ reacts with Trp as it would have non-identical binding sites. We evaluate that one binding site for Trp is as for free repressor and the second is as for repressor–DNA binding pocket. Since Trp dissociates much faster from the free repressor (see the section Kinetic parameter estimation) and the repressor–operator complex with one molecule of Trp at the repressor–DNA-like binding pocket will predominate the second state, we made the following approximation: first, dissociate the Trp molecule from the free-repressor-like binding pocket. The assumption of non-identical binding sites of the third repressor is justified by the following observation. X-ray studies[33] of the holorepressor–operator complex showed that the molecule of Trp makes a hydrogen bond with the cytosine base, which is in another strand of DNA two bases farther from the GNACT half-site. In Fig. 1, one can notice that after all half-sites, there are bases of cytosine with one exception of the third repressor binding site close to the RNAP binding site! At present, the calculated value of $K_3^{(3)}$ is in the range between binding of aporepressor to specific and non-specific sites on DNA.[46]

## Kinetic parameter estimation

First we assign values to kinetic parameters for repressor binding/unbinding to successive sites on the operator. The assignment of reaction rate constants to proposed reaction schemes is presented in Fig. 7. The values of these parameters are collected in Table 3. Since mainly dissociation rate constants were determined experimentally, we calculated the association rate constants from dissociation constants given in Table 2. The results of SPR experiments[48,66] of holorepressor binding pointed out that if the operator is occupied only with one holorepressor, this holorepressor dissociates fast. However, if the second holorepressor is bound with the operator, it dissociates very slowly. Hurlburt and Yanofsky[50] measured the dissociation rate of the repressor–operator system as a function of Trp concentration (for experimental details, see Fig. 5 in Hurlburt and Yanofsky[50] and Supplementary Material). In the light of results from SPR experiments of repressor–operator decay, it is clear that observed decay results from detachment of the second repressor. Therefore, we performed a fit to their data to obtain dissociation constants for the second repressor $k_3^{(2)}$, $k_7^{(2)}$, $k_9^{(2)}$ (see Supplementary Material for details of the fitting procedure). Since the affinity of the repressors to the third binding site is much lower, its role in the promoter blocking is weaker compared with $O^{(1)}$ and $O^{(2)}$. Therefore, estimation of these parameters is not crucial for the functioning of the switch. Moreover, these parameter values were not determined in experiments. We simply assume that the association rate constant of the third repressor is of the order of the rate constants for the second repressor (the second repressor binding appears to be insensitive to a number of Trp molecules that it contains).

The maximum rate of transcription initiation for *trp* operon was measured[68] to be equal to 5.1 transcripts per minute. Therefore, the time needed for binding of RNAP with promoter, transition

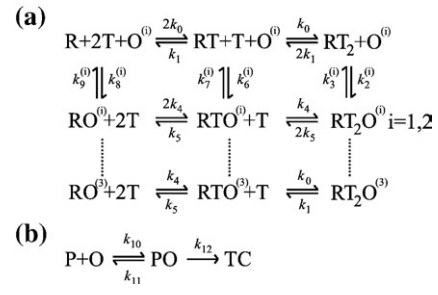


**Fig. 7.** (a) Reaction rate constants for the reaction schemes presented in Fig. 6. (b) RNAP binding with promoter. O stands for promoter, i.e., all sites $O^{(1),(2),(3)}$ are free.

**Table 4.** Miscellaneous parameters

| Symbol | Value | Reference |
|---|---|---|
| $[R_{tot}]$ | 120 m. m.+Trp | Gunsalus *et al.*[60] |
| $[T_{tot}]$ | $2.62\times10^4$ m. m. | Bliss[72] |
| $[P]^a$ | 144 | Bremer *et al.*[73] |
| $[O_{tot}]$ | 1 | |
| $V_{cell}$ ($\mu m^3$) | 1 | |

m. m., bacteria growing in minimal medium; +Trp, with tryptophan. Concentrations are expressed in molecules per cubic micrometer.
[a] Concentration of free functional RNAP.

through all intermediates to open complex and promoter clearance is equal to 11.8 s. Figure 7b depicts an assumed scheme of reactions for RNAP action. Promoter clearance takes about 1 s.[69,70] Since *trp* promoter belongs to a family of strong promoters, we assume that the association rate constant $k_{10}$ is similar to that determined by Sclavi *et al.*[67] for another promoter. Relying on the work of Mulligan *et al.*,[71] we calculated that $k_{10}/k_{11}k_{12}=3.65\times10^{-3}$ $\mu m^3\cdot molecules^{-1}\cdot s^{-1}$. Therefore, knowledge of the concentration of free RNAP in the cell (see Table 4) allows calculation of $k_{11}$, $k_{12}$, assuming reaction schemes considered in this work for $[T]=0$ and that the appearance of the transcribing complex needs 10.8 s.

### Remaining parameters

Consumption of Trp in the bacterium is commonly modeled using Michaelis–Menten relation.[5–10] We follow these works and describe the process of Trp consumption by the following relation

$$T\rightarrow\emptyset, \qquad \text{with rate } V_{max}[T]/(K+[T]) \quad (21)$$

$V_{max}$ stands for maximum Trp consumption, while $K$ is the concentration of Trp at which the rate of consumption is half its maximum. These parameters were estimated for steady-state case[10] and found equal to $V_{max}=2400$ molecules/(cell s) and $K=6000$ molecules per cell. If Trp level decreases, the pool of $tRNA^{Trp}$ decreases as well and the rate of Trp consumption slows. Although the relation given by Eq. (21) describes well Trp consumption close to the steady state, it overestimates the rate of Trp incorporation for low concentrations of this amino acid. For simplicity, we assume that value of the $V_{max}$ is one-tenth of the steady state.[5] If the initial number of Trp molecules is 50,000 per bacterium cell, the whole Trp disappears after about 500 s if it is not synthesized by the bacterium. For simplicity, we assume that total operator concentration is 1 molecule per cell (there is only one operator copy number per cell) and the volume of the cell is constant and equal to 1 $\mu m^3$. The total concentration of other species is given in Table 4. Only the concentration of Trp in the cells of bacteria growing in minimal media without Trp was determined experimentally. The intracellular Trp concentration for bacteria growing on medium rich in Trp is higher. Therefore, we start our derepression experiments with the concentration of Trp equal to 50,000 molecules per cell. For such concentration, the RNAP is unable to bind with the promoter.

## Acknowledgements

H and MT acknowledge the Foundation for Polish Science for the scholarship MISTRZ. This work was supported by a grant 2006-2008 from the budget for science of MNiSzW.

## Supplementary Data

Supplementary data associated with this article can be found, in the online version, at doi:10.1016/j.jmb.2008.01.060

## References

1. Khodursky, A. B., Peter, B. J., Cozzarelli, N. R., Botstein, D., Brown, P. O. & Yanofsky, C. (2000). DNA microarray analysis of gene expression in response to physiological and genetic changes that affect tryptophan metabolism in *Escherichia coli*. *Proc. Natl Acad. Sci. USA*, **97**, 12170–12175.
2. Yanofsky, C. & Horn, V. (1994). Role of regulatory features of the *trp* operon of *Escherichia coli* in mediating a response to a nutritional shift. *J. Bacteriol.* **176**, 6245–6254.
3. Yanofsky, C. & Crawford, I. P. (1987). The tryptophan operon. In *Escherichia coli* and *Salmonella typhimurium*: Cellular and Molecular Biology (Neidhart, F. C., ed), pp. 1454–1472, ASM Press, Washington, DC.
4. Yanofsky, C., Kelley, R. L. & Horn, V. (1984). Repression is relieved before attenuation in the *trp* operon of *Escherichia coli* as tryptophan starvation becomes increasingly severe. *J. Bacteriol.* **158**, 1018–1024.
5. Santillan, M. & Mackey, M. C. (2001). Dynamic regulation of the tryptophan operon: a modeling study and comparison with experimental data. *Proc. Natl Acad. Sci. USA*, **98**, 1364–1369.
6. Santillan, M. & Mackey, M. C. (2001). Dynamic behavior in mathematical models of the tryptophan operon. *Chaos*, **11**, 261–268.
7. Santillan, M. & Zeron, E. S. (2004). Dynamic influence of feedback enzyme inhibition and transcription attenuation on the tryptophan operon response to nutritional shifts. *J. Theor. Biol.* **231**, 287–298.
8. Bhartiya, S., Rawool, S. & Venkatesh, K. V. (2003). Dynamic model of *Escherichia coli* tryptophan operon shows an optimal structural design. *Eur. J. Biochem.* **270**, 2644–2651.
9. Drozdov-Tikhomirov, L. N. & Scoorida, G. I. (1977). Mathematical model for the kinetic of tryptophan synthesis and excretion by the cell of *E. coli*. *Mol. Biol. (Moscow)*, **11**, 843–853.
10. Bliss, R. D., Painter, P. R. & Marr, A. G. (1982). Role of feedback inhibition in stabilizing the classical operon. *J. Theor. Biol.* **97**, 177–193.
11. Sinha, S. (1986). Theoretical study of tryptophan

operon: application in microbial technology. *Biotechnol. Bioeng.* **31**, 117–124.
12. Koh, B. T. & Yap, M. G. (1993). A simple genetically structured model of *trp* repressor–operator interactions. *Biotechnol. Bioeng.* **41**, 707–714.
13. Koh, B. T., Tan, R. B. H. & Yap, M. G. S. (1998). Genetically structured mathematical modeling of *trp* attenuator mechanism. *Biotechnol. Bioeng.* **58**, 502–509.
14. Xiu, Z. L., Zeng, A. P. & Deckwer, W. D. (1997). Model analysis concerning the effects of growth rate and intracellular tryptophan level on the stability and dynamics of tryptophan biosynthesis in bacteria. *J. Biotechnol.* **58**, 125–140.
15. Rose, J. K. & Yanofsky, C. (1974). Interaction of the operator of the tryptophan operon with repressor. *Proc. Natl Acad. Sci. USA*, **71**, 3134–3138.
16. Sigler, P. B. (1992). The molecular mechanism of *trp* repression. In *Transcriptional Regulation* (McKnight, S. L. & Yamamoto, K. R., eds), pp. 475–498, Cold Spring Harbor Laboratory Press, Cold Spring Harbor, NY.
17. Jackson, E. N. & Yanofsky, C. (1973). The region between the operator and first structural gene of the tryptophan operon of *Escherichia coli* may have a regulatory function. *J. Mol. Biol.* **76**, 89–101.
18. Yanofsky, C. (1981). Attenuation in the control of expression of bacterial operons. *Nature*, **289**, 751–758.
19. Squires, C. L., Lee, F. D. & Yanofsky, C. (1975). Interaction of the *trp* repressor and RNA polymerase with the *trp* operon. *J. Mol. Biol.* **92**, 93–111.
20. Gunsalus, R. P. & Yanofsky, C. (1980). Nucleotide sequence and expression of *Escherichia coli* trpR, the structural gene for the trp aporepressor. *Proc. Natl Acad. Sci. USA*, **77**, 7117–7121.
21. Joachimiak, A., Kelley, R. L., Gunsalus, R. P., Yanofsky, C. & Sigler, P. B. (1983). Purification and characterization of *trp* aporepressor. *Proc. Natl Acad. Sci. USA*, **80**, 668–672.
22. Somerville, R. (1992). The Trp repressor, a ligand-activated regulatory protein. *Prog. Nucleic Acid Res. Mol. Biol.* **42**, 1–38.
23. Arvidson, D. N., Bruce, C. & Gunsalus, R. P. (1986). Interaction of the *Escherichia coli trp* aporepressor with its ligand, L-tryptophan. *J. Biol. Chem.* **261**, 238–243.
24. Lane, A. N. (1986). The interaction of the *trp* repressor from *Escherichia coli* with L-tryptophan and indole propanoic acid. *Eur. J. Biochem.* **157**, 405–413.
25. Marmorstein, R. Q., Joachimiak, A., Sprinzl, M. & Sigler, P. B. (1987). The structural basis for the interaction between L-tryptophan and the *Escherichia coli trp* aporepressor. *J. Biol. Chem.* **262**, 4922–4927.
26. Jin, L., Yang, J. & Carey, J. (1993). Thermodynamics of ligand binding to *trp* repressor. *Biochemistry*, **32**, 7302–7309.
27. Schevitz, R. W., Otwinowski, Z., Joachimiak, A., Lawson, C. L. & Sigler, P. B. (1985). The three-dimensional structure of *trp* repressor. *Nature*, **317**, 782–786.
28. Zhang, R. G., Joachimiak, A., Lawson, C. L., Schevitz, R. W., Otwinowski, Z. & Sigler, P. B. (1987). The crystal structure of *trp* aporepressor at 1.8 Å shows how binding tryptophan enhances DNA affinity. *Nature*, **327**, 591–597.
29. Lawson, C. L., Zhang, R. G., Schevitz, R. W., Otwinowski, Z., Joachimiak, A. & Sigler, P. B. (1988). Flexibility of the DNA-binding domains of *trp* repressor. *Proteins*, **3**, 18–31.
30. Arrowsmith, C., Pachter, R., Altman, R. & Jardetzky, O. (1991). The solution structures of *Escherichia coli trp* repressor and *trp* aporepressor at an intermediate resolution. *Eur. J. Biochem.* **202**, 53–66.
31. Zhao, D., Arrowsmith, C. H., Jia, X. & Jardetzky, O. (1993). Refined solution structures of the *Escherichia coli trp* holo- and aporepressor. *J. Mol. Biol.* **229**, 735–746.
32. Ramesh, V., Frederick, R. O., Syed, S. E., Gibson, C. F., Yang, J. C. & Roberts, G. C. (1994). The interactions of *Escherichia coli trp* repressor with tryptophan and with an operator oligonucleotide. NMR studies using selectively $^{15}$N-labelled protein. *Eur. J. Biochem.* **225**, 601–608.
33. Otwinowski, Z., Schevitz, R. W., Zhang, R. G., Lawson, C. L., Joachimiak, A., Marmorstein, R. Q. *et al.* (1988). Crystal structure of *trp* repressor/operator complex at atomic resolution. *Nature*, **335**, 321–329.
34. Zhang, H., Zhao, D., Revington, M., Lee, W., Jia, X., Arrowsmith, C. & Jardetzky, O. (1994). The solution structures of the *trp* repressor–operator DNA complex. *J. Mol. Biol.* **238**, 592–614.
35. Lawson, C. L. & Carey, J. (1993). Tandem binding in crystals of a *trp* repressor/operator half-site complex. *Nature*, **366**, 178–182.
36. Kumamoto, A. A., Miller, W. G. & Gunsalus, R. P. (1987). *Escherichia coli* tryptophan repressor binds multiple sites within the aroH and *trp* operators. *Genes Dev.* **1**, 556–564.
37. Liu, Y. C. & Matthews, K. S. (1993). Dependence of *trp* repressor–operator affinity, stoichiometry, and apparent cooperativity on DNA sequence and size. *J. Biol. Chem.* **268**, 23239–23249.
38. Yang, J., Gunasekera, A., Lavoie, T. A., Jin, L. H., Lewis, D. E. A. & Carey, J. (1996). *In vivo* and *in vitro* studies of TrpR–DNA interactions. *J. Mol. Biol.* **258**, 37–52.
39. Joachimiak, A., Haran, T. E. & Sigler, P. B. (1994). Mutagenesis supports water mediated recognition in the *trp* repressor–operator system. *EMBO J.* **13**, 367–372.
40. Brown, M. P., Grillo, A. O., Boyer, M. & Royer, C. A. (1999). Probing the role of water in the tryptophan repressor–operator complex. *Protein Sci.* **8**, 1276–1285.
41. Bareket-Samish, A., Cohen, I. & Haran, T. E. (1997). Repressor assembly at *trp* binding sites is dependent on the identity of the intervening dinucleotide between the binding half sites. *J. Mol. Biol.* **267**, 103–117.
42. Bareket-Samish, A., Cohen, I. & Haran, T. E. (1998). Direct *versus* indirect readout in the interaction of the *trp* repressor with non-canonical binding sites. *J. Mol. Biol.* **277**, 1071–1080.
43. Haran, T. E., Joachimiak, A. & Sigler, P. B. (1992). The DNA target of the *trp* repressor. *EMBO J.* **11**, 3021–3030.
44. Liu, Y. C. & Matthews, K. S. (1994). *Trp* repressor mutations alter DNA complex stoichiometry. *J. Biol. Chem.* **269**, 1692–1698.
45. Jeeves, M., Evans, P. D., Parslow, R. A., Jaseja, M. & Hyde, E. I. (1999). Studies of the *Escherichia coli* Trp repressor binding to its five operators and to variant operator sequences. *Eur. J. Biochem.* **265**, 919–928.
46. Grillo, A. O., Brown, M. P. & Royer, C. A. (1999). Probing the physical basis for *trp* repressor–operator recognition. *J. Mol. Biol.* **287**, 539–554.
47. Hurlburt, B. K. & Yanofsky, C. (1990). Enhanced operator binding by *trp* superrepressors of *Escherichia coli*. *J. Biol. Chem.* **265**, 7853–7858.
48. Finucane, M. D. & Jardetzky, O. (2003). Surface plasmon resonance studies of wild-type and AV77 tryptophan repressor resolve ambiguities in superrepressor activity. *Protein Sci.* **12**, 1613–1620.
49. Chou, W. Y., Bieber, C. & Matthews, K. S. (1989).

Tryptophan and 8-anilino-1-naphthalenesulfonate compete for binding to *trp* repressor. *J. Biol. Chem.* **264**, 18309–18313.
50. Hurlburt, B. K. & Yanofsky, C. (1992). *trp* repressor/*trp* operator interaction. Equilibrium and kinetic analysis of complex formation and stability. *J. Biol. Chem.* **267**, 16783–16789.
51. Lee, W., Revington, M., Farrow, N. A., Nakamura, A., Utsunomiya-Tate, N., Miyake, Y. *et al.* (1995). Rapid corepressor exchange from the trp-repressor/operator complex: an NMR study of [ul-$^{13}$C/$^{15}$N]-L-tryptophan. *J. Biomol. NMR*, **5**, 367–375.
52. Gillespie, D. T. (1976). A general method for numerically simulating the stochastic time evolution of coupled chemical reactions. *J. Comput. Phys.* **22**, 403–434.
53. van Kampen, N. G. (1997). *Stochastic processes in physics and chemistry.* Elsevier, Amsterdam.
54. Gillespie, D. T. (1992). A rigorous derivation of the chemical master equation. *Phys. A*, **188**, 404–425.
55. Hurlburt, B. K. & Yanofsky, C. (1993). Analysis of heterodimer formation by the *Escherichia coli trp* repressor. *J. Biol. Chem.* **268**, 14794–14798.
56. Reedstrom, R. J., Brown, M. P., Grillo, A., Roen, D. & Royer, C. A. (1997). Affinity and specificity of *trp* repressor–DNA interactions studied with fluorescent oligonucleotides. *J. Mol. Biol.* **273**, 572–585.
57. Carey, J. (1988). Gel retardation at low pH resolves *trp* repressor–DNA complexes for quantitative study. *Proc. Natl Acad. Sci. USA*, **85**, 975–979.
58. Czernik, P. J., Shin, D. S. & Hurlburt, B. K. (1994). Functional selection and characterization of DNA binding sites for *trp* repressor of *Escherichia coli*. *J. Biol. Chem.* **269**, 27869–27875.
59. Klig, L. S., Crawford, I. P. & Yanofsky, C. (1987). Analysis of *trp* repressor–operator interaction by filter binding. *Nucleic Acids Res.* **15**, 5339–5351.
60. Gunsalus, R. P., Miguel, A. G. & Gunsalus, G. L. (1986). Intracellular Trp repressor levels in *Escherichia coli*. *J. Bacteriol.* **167**, 272–278.
61. Gibson, M. A. & Bruck, J. (2000). Efficient exact stochastic simulation of chemical systems with many species and many channels. *J. Phys. Chem. A*, **104**, 1876–1889.
62. Chatterjee, S., Zhou, Y. N., Roy, S. & Adhya, S. (1997). Interaction of Gal repressor with inducer and operator: induction of *gal* transcription from repressor-bound DNA. *Proc. Natl Acad. Sci. USA*, **94**, 2957–2962.
63. Swint-Kruse, L., Zhan, H. & Matthews, K. S. (2005). Integrated insights from simulation, experiment, and mutational analysis yield new details of LacI function. *Biochemistry*, **44**, 11201–11213.
64. van Zon, J. S., Morelli, M. J., Tănase-Nicola, S. & ten Wolde, P. R. (2006). Diffusion of transcription factors can drastically enhance the noise in gene expression. *Biophys. J.* **91**, 4350–4367.
65. Schmitt, T. H., Zheng, Z. & Jardetzky, O. (1995). Dynamics of tryptophan binding to *Escherichia coli* Trp repressor wild type and AV77 mutant: an NMR study. *Biochemistry*, **34**, 13183–13189.
66. Jardetzky, O. & Finucane, M. D. (2007). Tandem interactions in the *trp* repressor system may regulate binding to operator DNA. In Structure and Biophysics—New Technologies for Current Challenges in Biology and Beyond (Puglisi, J. D., ed) pp. 49–64, Springer Netherlands, Dordrecht, the Netherlands.
67. Sclavi, B., Zaychikov, E., Rogozina, A., Walther, F., Buckle, M. & Heumann, H. (2005). Real-time characterization of intermediates in the pathway to open complex formation by *Escherichia coli* RNA polymerase at the T7A1 promoter. *Proc. Natl Acad. Sci. USA*, **102**, 4706–4711.
68. Baker, R. & Yanofsky, C. (1972). Transcription initiation frequency and translational yield for the tryptophan operon of *Escherichia coli*. *J. Mol. Biol.* **69**, 89–102.
69. McClure, W. R. (1985). Mechanism and control of transcription initiation in prokaryotes. *Annu. Rev. Biochem.* **54**, 171–204.
70. Record, M. T. J., Reznikoff, W. S., Craig, M. L., McQuade, K. L. & Schlax, P. J. (1996). *Escherichia coli* RNA polymerase ($E\sigma^{70}$), promoters, and the kinetics of the steps of transcription initiation. In Escherichia coli and *Salmonella typhimurium*: Cellular and Molecular Biology (Neidhart, F. C., ed), pp. 792–821, ASM Press, Washington, DC.
71. Mulligan, M. E., Hawley, D. K., Entriken, R. & McClure, W. R. (1984). *Escherichia coli* promoter sequences predict *in vitro* RNA polymerase selectivity. *Nucleic Acids Res.* **12**, 789–800.
72. Bliss, R. D. (1979). A specific method for determination of free tryptophan and endogenous tryptophan in *Escherichia coli*. *Anal. Biochem.* **93**, 390–398.
73. Bremer, H., Dennis, P. & Ehrenberg, M. (2003). Free RNA polymerase and modeling global transcription in *Escherichia coli*. *Biochimie*, **85**, 597–609.